DOI: 10.1002/ejic.200600571

Lithium Oligophosphanediides in the Li/$PhPCl_2$ System

Daniel Stein,[a] Alk Dransfeld,[b] Michaela Flock,[b] Heinz Rüegger,[a] and Hansjörg Grützmacher*[a]

Keywords: Alkali metals / Dianions / Ion pairs / NMR spectroscopy / Phosphorus / Reduction

Optimized conditions for the selective synthesis of $[Li_2(P_nPh_n)(tmeda)_x]$ (n = 2, 3, 4) have been developed. X-ray diffraction with single crystals show $[Li_2(P_2Ph_2)(tmeda)_2]$ and $[Li_2(P_4Ph_4)(tmeda)_2]$ to be ion triples, while for n = 3 the ion pair $[Li(tmeda)_2]^+[Li(P_3Ph_3)(tmeda)]^-$ is observed. NMR experiments support the assumption that these structures are retained in solution. Structural differences between the lithium and the corresponding sodium compounds, $[Na_2(P_nPh_n)(tmeda)_x]$, can be partially rationalized using the electrostatic stabilization parameters, ESP = $\Sigma(1/r_{M^+,M^+}) + \Sigma(1/r_{P^-,P^-}) - \Sigma(1/r_{M^+,P^-})$; M = Li, Na.

Introduction

Dichlorophenylphosphane ($PhPCl_2$; also known as phenylphosphonous acid dichloride) is a versatile starting material in organophosphorus chemistry that is produced on a large scale from PCl_3 and benzene.[1] Its reductive dehalogenation reaction with alkali metals (M) to give cyclic oligo(phenyl)phosphanes, $(PhP)_n$ (n = 3–6) has been investigated.[2a–2j] Further reaction of $(PhP)_n$ with strongly reducing metals (M = Li, Na, or K) leads to reductive bond cleavage (RBC) and formation of alkali metal *catena*-oligophosphane-α,ω-diides, $[M_2(P_nPh_n)(solv)_x]$.[2a,2b,3] In their pioneering work, Caulton[3a] and Baudler[3b,3c] were able to obtain some structural information about the dimetal 1,2,3-triphenyltriphosphane-1,3-diides $[M_2(P_3Ph_3)(solv)_x]$ and the 1,2,3,4-tetraphenyltetraphosphane-1,4-diides $[M_2(P_4Ph_4)(solv)_x]$ from ^{31}P NMR spectroscopy in solution. Recently, Hey-Hawkins et al.[4] and ourselves[5a–5c] have succeeded in the crystallization of various sodium *catena*-oligophosphane-α,ω-diides, namely 1,2-diphenyldiphosphane-1,2-diide $[Na_6(P_2Ph_2)_3(dme)_3]$ (**I**),[5a] 1,2,3-triphenyltriphosphane-1,3-diide $[Na_2(P_3Ph_3)(tmeda)_3]$ (**II**),[5a] and the 1,2,3,4-tetraphenyltetraphosphane-1,4-diides $[Na_2(P_4Ph_4)(tmeda)_2]$ (**IIIa**),[5a] $[Na_2(P_4Ph_4)(dme)_3]$ (**IIIb**),[5a] $[Na_2(P_4Ph_4)(thf)_4(tmu)]$ (**IIIc**),[5b] and $[Na_2(P_4Ph_4)(thf)_5]$ (**IIId**) (tmeda = tetramethylethylenediamine, tmu = tetramethylurea), which can be isolated from the $PhPCl_2$/Na system in organic solvents.[4] Figure 1 summarizes these results.

Compound **I** consists of a $[Na(dme)_3]^+$ cation and the cluster anion $[Na_5(P_2Ph_2)_3(dme)_3]^-$ (see Figure 1a for a schematic representation and Figure 1b for a space-filling model). The structure of **II** is shown in Figure 1 (c and d), parts e and f show the structure of **IIIa** as a representative of all $[M_2(P_4Ph_4)(solv)_n]$ compounds. A solvent molecule acts as bridging ligand L (L = dme, tmu, or thf) between the two Na^+ ions in **IIIb**–**d**. In the schematic pictures of the structures of **I**, **II**, and **III**, a plus sign is placed at the position of the sodium cations and a minus sign at the terminal phosphorus centers of the dianionic $(P_nPh_n)^{2-}$ chains. Compounds **II** and **III** are classical *ion triples* (two cations, one dianion). The cluster anion in **I** may be viewed as a cyclic trimer of a corner-sharing ion triple that is additionally capped by two sodium cations on the top and bottom of the central hexagonal P_6 prism. With the structural parameters of these ionic aggregates, the electrostatic stabilization parameter (ESP) given by Equation (1) was calculated. The resulting data are listed in Table 1.

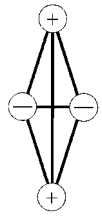

$$\mathrm{ESP} = \sum \frac{1}{r_{+,-}} + \sum \frac{1}{r_{-,-}} - \sum \frac{1}{r_{+,}} \quad (1)$$

The ESP was introduced by Streitwieser Jr. to account for the amazingly high stability of ion triples in carbanion chemistry[6] and is simply the sum of the repulsive interactions between like charges, expressed by $(1/r_{+,+})$ and

[a] Department of Chemistry and Applied Biosciences, HCI, ETH Hönggerberg,
8093 Zürich, Switzerland,
Fax: +41-1-632-1032
E-mail: gruetzmacher@inorg.chem.ethz.ch
[b] Institut für Anorganische Chemie der TU Graz,
8010 Graz, Austria
E-mail: alk.dransfeld@tugraz.at

Supporting information for this article is available on the WWW under http://www.eurjic.org or from the author.

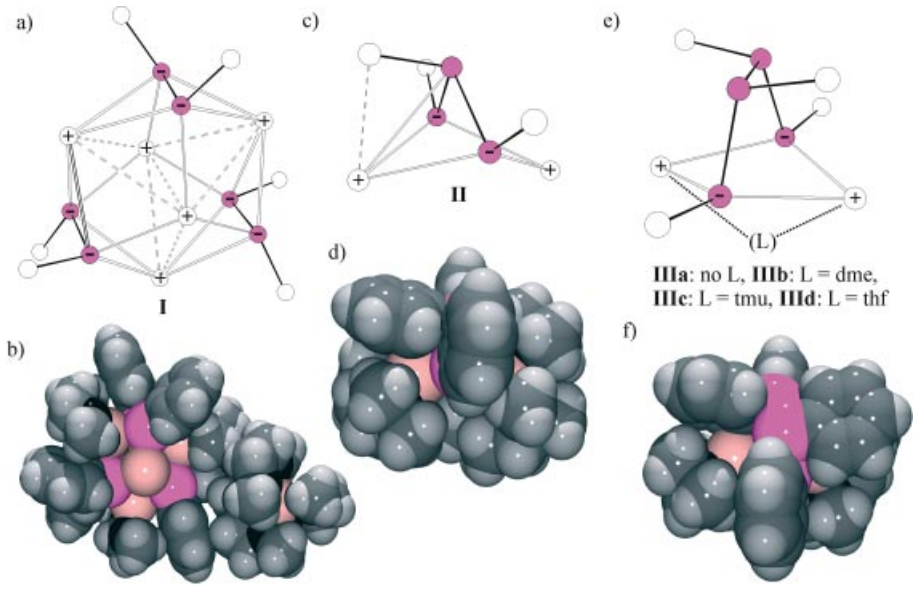

Figure 1. Schematic representations and space-filling plots of $[Na_5(P_2Ph_2)_3]^-$ (a, b), $[Na_2(P_3Ph_3)]$ (c, d), and $[Na_2(P_4Ph_4)(L)]$ (e, f).

Table 1. Repulsive interactions $r(Na^+Na^+)$ and $r(P^-P^-)$ [Å] and attractive interactions $r(Na^+P^-)$ [Å] and the resulting ESPs [$Å^{-1}$] for **I**, **II**, and **IIIa**–**c**. L indicates a bridging dme or tmu ligand between the Na^+ ions.

	$[Na_5(P_2Ph_2)_3]^-$ **I**	$[Na_2(P_3Ph_3)]$ **II**	$[Na_2(P_4Ph_4)]$ **IIIa**	$[Na_2(P_4Ph_4)L]$ **IIIb**	$[Na_2(P_4Ph_4)L]$ **IIIc**
$r(Na^+Na^+)$	3.669(7) × 6	4.781(1)	4.587(5)	3.519(6)	3.491(4)
	3.96(1) × 1				
	5.35(1) × 3				
$r(P^-P^-)$	2.20(1) × 3	3.146(1)	3.406(3)	3.947(4)	3.475(2)
	4.66(1) × 6				
	5.10(1) × 6				
$r(Na^+P^-)$	3.063(6) × 6	2.968(1)	2.848(4)	2.916(6)	2.974(2) × 2
	3.158(7) × 6	2.966(1)	2.885(4)	2.933(6)	2.918(2) × 2
	2.831(5) × 6	3.106(1)	2.829(4)	2.960(6)	
	4.092(7) × 6	3.097(1)	2.972(5)	2.849(6)	
ESP	–1.17	–0.79	–0.87	–0.84	–0.77

$(1/r_{-,-})$, minus the sum of attractive interactions, expressed by $(1/r_{+,-})$. Despite the fact that the ESP treats the ions simply as point charges and completely neglects steric interactions and solvation energies, it can be used to interpret the stability of ion pairs qualitatively. For example, the high negative ESP value for **I** explains why the structure of this cluster is also maintained in solution.[5a] The ESP also indicates that ion pairs with the $(P_3Ph_3)^{2-}$ dianion like **II** may be labile because of the rather short P1···P3 distance (ca. 3.15 Å) and the significantly longer Na–P distances. These are caused by repulsive steric interactions between the phenyl groups, especially the one at the central phosphorus atom, and the solvent molecules coordinated to Na^+. In structures with the $(P_4Ph_4)^{2-}$ dianion, the steric encumbrance is less pronounced and the Na^+–P^- distances are shorter, which leads to more negative ESPs.

Only in **IIIc**, which contains a bridging tmu molecule and a strongly folded Na_2P_2 ring, is the Na^+–Na^+ distance more than 1 Å shorter than in **IIIa** (no bridging L); as a result the electrostatic stabilization is slightly less than that of **II**.

The motivation for this work was i) to find reliable conditions for the synthesis and isolation of the dilithium(*catena*-oligophosphane-α,ω-diides) $[Li_2(P_nPh_n)(solv)_x]$ (here and further on x stands for an unspecified number of solvent molecules), ii) to determine their solid-state structures, and iii) to make, whenever possible, proposals for their behavior in solution. We focused on the isolation of compounds with tmeda as co-ligand for Li^+ in order to obtain a set of comparable compounds.

Results and Discussion

Syntheses

The syntheses that worked best in our hands and gave good yields of pure isolated and crystalline material are outlined in Scheme 1. In a reductive bond cleavage (RBC) reaction, pentaphenylcyclopentaphosphane (**1**)[2i] was treated with an excess of lithium powder in THF. The resulting orange-red solution showed only one signal at δ =

–102.9 ppm in the ^{31}P NMR spectrum, thus indicating the formation of the P_2^{2-} dianion. The primary product, $[Li_2(P_2Ph_2)(thf)_x]$ (**2′**) was obtained as red powder after evaporation of the solvent. Subsequent recrystallization of **2′** from hot toluene/tmeda (2:1 by vol.) gave red crystals of $[Li_2(P_2Ph_2)(tmeda)_2]$ (**2**).

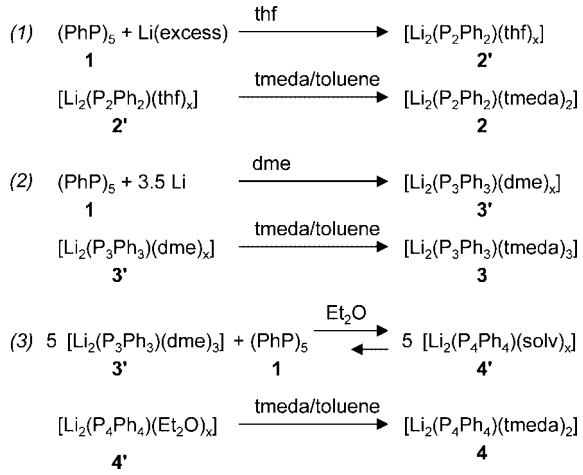

Scheme 1. Syntheses of isolable dilithium(*catena*-oligophosphane-α,ω-diides), $[Li_2(P_nPh_n)(tmeda)_m]$ **2** (n = 2, m = 2), **3** (n = 3, m = 3), and **4** (n = 4, m = 2).

The best synthesis for dilithium 1,2,3-triphenyltriphosphane-1,3-diide (**3**) was found to be the reaction of $(PhP)_5$ with a stoichiometric amount of lithium in dme as reaction medium. In this solvent, the product $[Li_2(P_3Ph_3)(dme)_x]$ (**3′**) precipitates directly from the reaction mixture as a bright-orange powder in good yield (about 70%). The content of dme (x = 2–3) was estimated by NMR spectroscopy. Subsequently, **3′** was dissolved in a 5:1 mixture of toluene and tmeda and this solution was concentrated to dryness under high vacuum to remove all volatiles, especially dme; the resulting yellow powder was recrystallized at 7 °C from toluene to give yellow crystals of the composition $[Li_2(P_3Ph_3)(tmeda)_3]$ (**3**).

The best method for the synthesis of pure dilithium 1,2,3,4-tetraphenyltetraphosphane-1,4-diide (**4**) turned out to be the stoichiometric reaction of **3′** with $(PhP)_5$ (**1**) in diethyl ether. After removal of all volatiles under vacuum, the resulting orange powder (**4′**) of composition $[Li_2(P_4Ph_4)(solv)_x]$ (solv = Et_2O, dme) was dissolved in a 10:3 mixture of toluene and tmeda, again concentrated to dryness under vacuum, and then recrystallized from methyl *tert*-butyl ether (mtbe) to give slightly yellow crystals of the composition $[Li_2(P_4Ph_4)(tmeda)_2]$ (**4**). Attempts to synthesize **4′** or **4** by a direct RBC reaction of **1** with the corresponding amount of lithium gave a lower yield (<50%).

Structures

The structures of the dilithium *catena*-oligophosphane-α,ω-diides $[Li_2(P_nPh_n)]$ (n = 2–4) were investigated by X-ray diffraction studies. All compounds contain tmeda molecules as co-ligands bonded to the lithium ions. The Li^+Li^+, P^-P^-, and Li^+P^- distances in **2**, **3**, and **4** are listed in Table 2.

The centrosymmetric structure of **2** (Figure 2) can be viewed as the archetypical structure of an ion triple with two formal negative charges in the α-position of the dianion. The P–P distance [2.244(3) Å] is slightly longer than the comparable one in the sodium compound [2.20(1) Å]. The main structural difference resides in the orientation of the phenyl rings, which are in a *trans* arrangement in **2** while they take a gauche conformation in the cluster anion $[Na_5(P_2Ph_2)_3]^-$ of **I** (the C–P–P–C torsion angle is about –72°[5a]). The Ph–P–P–Ph moiety in **2** is planar. As a result of the short attractive Li^+–P^- interactions, the ESP for **2** (–0.94 Å^{-1}) is considerably more negative than the ESP (–0.72 Å^{-1}) for a hypothetical $[Na_2(P_2Ph_2)]$ ion triple with a structure analogous to that of **2** (an Na–P distance of 2.98 Å, which is the average of the data listed in Table 1, is assumed).

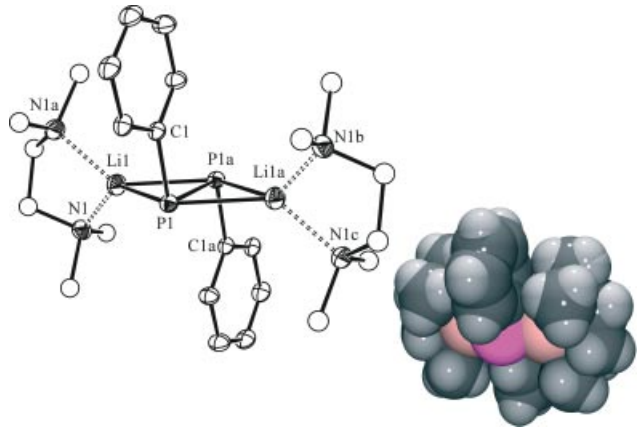

Figure 2. Structure of **2**. Selected distances [Å] and angles [°]: P1–P1 2.244(3), Li–P1 2.483(1), P1–C1 1.820(1), Li–N1 2.077(1); C1–P1–P1 98.66(2), C1–P1–Li 93.90(1), Li–P1–Li 126.28(3); torsion angles: Li–P1–LiA–P1A 0.0, P1A–P1–C1–C2 0.0, C1–P1–P1A–C1A 180.0.

In the solid state, **3** forms an *ion pair* composed of a $[Li(tmeda)_2]^+$ cation and an anionic *ion double*, namely $[Li(P_3Ph_3)(tmeda)]^-$. Only one lithium ion coordinates to the terminal phosphorus atoms P1 and P3 and, as expected for steric reasons, the coordination occurs from the opposite site to the central phenyl group at P2. The distance between the two terminal phosphorus atoms P1 and P3 in **2** is about 0.2 Å longer (the P–P–P angle is about 8° larger)

Table 2. Selected distances [Å] and the resulting ESPs for **2**–**4**.

	$[Li_2(P_2Ph_2)(tmeda)_2]$	$[Li(tmeda)_2]^+[Li(P_3Ph_3)(tmeda)]^-$	$[Li_2(P_4Ph_4)(tmeda)_2]$
$r(Li^+Li^+)$	4.430(2)	–	3.967(2)
$r(P^-P^-)$	2.244(3)	3.347(1)	3.229(2)
$r(Li^+P^-)$	2.483(1)×4	2.499(7), 2.525(7)	2.618(4)×2, 2.653(4)×2
ESP	–0.94	–0.50	–0.96

than in the neutral ion triple $[Na_2(P_3Ph_3)(tmeda)_3]$ (**II**), where two sodium ions coordinate to P1 and P3. The only other known triphosphanediide is found in the highly unstable ion pair $[Na(NH_3)_5]^+[Na(P_3H_3)(NH_3)_3]^-$, which contains the anionic ion double $[Na(P_3H_3)(NH_3)_3]^-$.[7] An even longer P^-–P^- distance (3.67 Å) and larger P–P–P angle (113.4°) is observed in this compound. An increase of the P^-–P^- distance will help to diminish the repulsive interactions in the ion doubles which, evidently, have less negative ESPs than the ion triples because of the long and hence less stabilizing Na–P distances {–0.79 $Å^{-1}$ for $[Na_2(P_3Ph_3)(tmeda)_3]$ **II**, –0.50 for $[Li(P_3Ph_3)(tmeda)]^-$, and only –0.37 for $[Na(P_3H_3)]^-$}. This loss of stabilizing electrostatic energy in the anionic ion doubles is compensated for by the solvation energy of the counter cations. Because these are much higher for lithium than for sodium,[8,9] the formation of an ion pair in the case of **3** and the formation of an ion triple for the sodium compound **II** is easily understood (Figure 3). Note that in the other ion pair, $[Na(NH_3)_5]^+[Na(P_3H_3)(NH_3)_3]^-$, the smaller size of the ammonia ligand compared to tmeda allows a higher coordination number at the sodium cations and a better solvation. Hence, the loss of ESP on going from the ion triple to the ion double can be compensated.

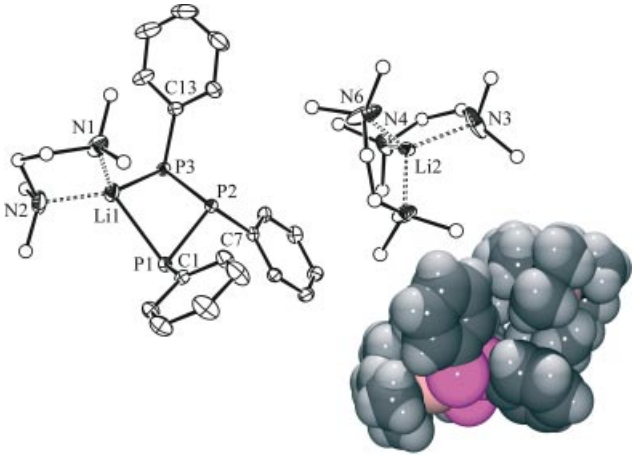

Figure 3. Structure of **3**. Selected distances [Å] and angles [°]: P1–P2 2.179(1), P2–P3 2.177(1), P1–C1 1.814(3), P2–C7 1.847(3), P3–C13 1.819(4), P1–Li1 2.493(7), P3–Li1 2.525(6), P1–P3 3.347(1), P1–P2–P3 100.02(5), P1–Li1–P3 83.37(2), C1–P1–P2 103.7(1), C7–P2–P3 105.8(1), C7–P2–P1 104.0(1), C13–P3–P2 102.8(1); torsion angles: C1–P1–P2–C7 106.7(2), C1–P1–P2–P3 40.9(2), C7–P2–P3–C13 112.9(2), C13–P3–P2–P1 139.3(1), Li1–P1–P2–C7 150.1(2), Li1–P3–P2–C7 148.2(2).

Finally, the structure of **4** was investigated. This compound has a composition very close to the corresponding sodium compound **IIIa** (both contain two tmeda molecules) and the solid-state structures are also very similar (Figure 4). Compounds **4** and **IIIa** are obtained as racemic mixtures and form ion triples in which the P_4 chain has either an (*R*,*R*)- or an (*S*,*S*)-configuration. Note the highly distorted coordination spheres around the lithium atoms and their contacts to the *ipso*-carbon atoms of the central phenyl rings. Both features are also observed in the sodium compound. However, due to the short Li^+–P^- distances, the ESP for this ion triple is rather high (–0.96 $Å^{-1}$).

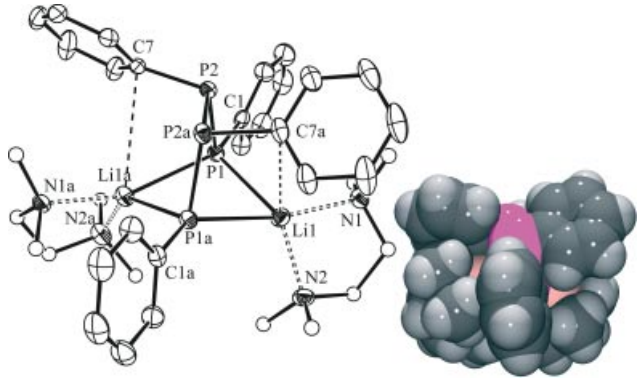

Figure 4. Structure of **4**. Selected distances [Å] and angles [°]: Li–P1 2.618(4), Li–P1A 2.652(4), Li–N1 2.144(4), Li–N2 2.095(5), P1–P2 2.167(1), P1–C1 1.832(2), P2–P2A 2.190(1), P2–C7 1.851(2); P1–Li–P1A 75.6(1), C1–P1–P2 102.26(9), P1–P2–P2A 103.37(2), P1–P2–C7 105.55(9), P2–P2A–C7A 99.70(8); torsion angles: P1–P2–P2A–P1A –13.3(1), C1–P1–P2–P2A –160.33(8), C1–P1–P2–C7 95.4(1), Li1–P1–P2–P2A –39.2(1), Li1A–P1A–P2A–P2 58.8(1).

The P–P distances for the $(P_2Ph_2)^{2-}$, $(P_3Ph_3)^{2-}$, and $(P_4Ph_4)^{2-}$ dianions are very similar in the lithium and sodium compounds. In the dianions of **2** and **I**, the P–P distance is greater than 2.2 Å, whereas in the dianions in **3** and **II** it is below 2.2 Å. The terminal P–P bonds in the $(P_4Ph_4)^{2-}$ dianions in **4** and **IIIa**–**d** are very slightly shorter (ca. 2.17 Å) than the central P–P bond (ca. 2.20 Å). The bonds between the formally negatively charged terminal phosphorus centers and the *ipso*-carbon atoms of the phenyl rings are a little shorter (by ca. 0.04 Å) in all compounds than the P–C_{ipso} bonds at the central phosphorus atoms. This observation may be taken as an indication of some delocalization of the negative charges into the phenyl groups, although this effect is small compared to amides.[10]

NMR Spectra

The compound $[Li_2(P_2Ph_2)(tmeda)_2]$ (**2**) is sparingly soluble in hydrocarbons but sufficiently soluble in $[D_8]$thf to obtain ^1H, ^{13}C, ^{31}P, and ^7Li NMR spectra. All data correspond quite closely with those observed for the sodium cluster anion $[Na_5(P_2Ph_2)_3(dme)_3]^-$ in **I**. The *ipso*-^{13}C carbon resonances of the phenyl groups are observed at δ = 162.2 ppm (δ = 160.7 ppm in **I**) and the ^{31}P NMR shifts also vary little (δ = –102.9 ppm in **2**, δ = –106.4 ppm in **I**). Unfortunately, the ^{31}P-^7Li couplings could not be resolved in the ^7Li NMR spectrum (broad signal at δ = 0.6 ppm). However, in view of the large loss of electrostatic stabilization energy upon dissociation of the ion triple into the ion pair $[Li(solv)_x][Li(P_2Ph_2)(solv)_y]$, we believe that the structure of **2** is retained in solution.

A $[D_8]$toluene solution of the salt $[Li(tmeda)_2]^+$-$[Li(P_3Ph_3)(tmeda)]^-$ (**3**) shows an AM_2 spin system with two multiplets centered at $\delta_A(^{31}P)$ = –52.3 ppm and $\delta_M(^{31}P)$ = –71.5 ppm. From a simulation of the spectrum, the coup-

ling constant $^1J_{A,M} \approx 224$ Hz was obtained. These data are very different from those for the sodium compound $[Na_2(P_3Ph_3)(tmeda)_3]$ (**II**), which shows an eight-line AB_2 spin system with $\delta_A = -54.0$ and $\delta_B = -56.7$ ppm ($^1J_{A,B}$ = 242 Hz). This finding indicates that different species containing the P_3Ph_3 unit are present in solution. The ^{7}Li NMR spectrum in [D$_8$]toluene at low temperature confirms this assumption: two signals are observed, one broad singlet at $\delta = 10.5$ ppm for the $[Li(tmeda)_2]^+$ cation and one broad multiplet at $\delta = 11.4$ ppm for the $[Li(P_3Ph_3)(tmeda)]^-$ anion, that is, **3** exists as an ion pair in solution, as observed in the solid state. That we could not resolve the ^{31}P-^{7}Li coupling is probably due to dynamic processes involving exchange of the Li-coordinated solvent molecules. On the contrary, the very different ^{31}P NMR chemical shifts for the sodium compound indicate that this forms an intact ion triple in solution.

The tetraphosphanediide $[Li_2(P_4Ph_4)(tmeda)_2]$ (**4**) is sufficiently soluble in [D$_8$]toluene to allow NMR measurements. At room temperature, ill-resolved multiplets at δ = –35 to –39 ppm and very broad signals at about $\delta \approx -76$ and $\delta \approx -95$ ppm are observed. At low temperature (248 K), two species (**4** and **4′′**) are observed in a 100:80 ratio in the ^{31}P NMR spectrum (see Figure 5, a). The major compound **4** shows two multiplets of an $AA'BB'X_2$ spin system in the ^{31}P NMR spectrum with chemical shifts at

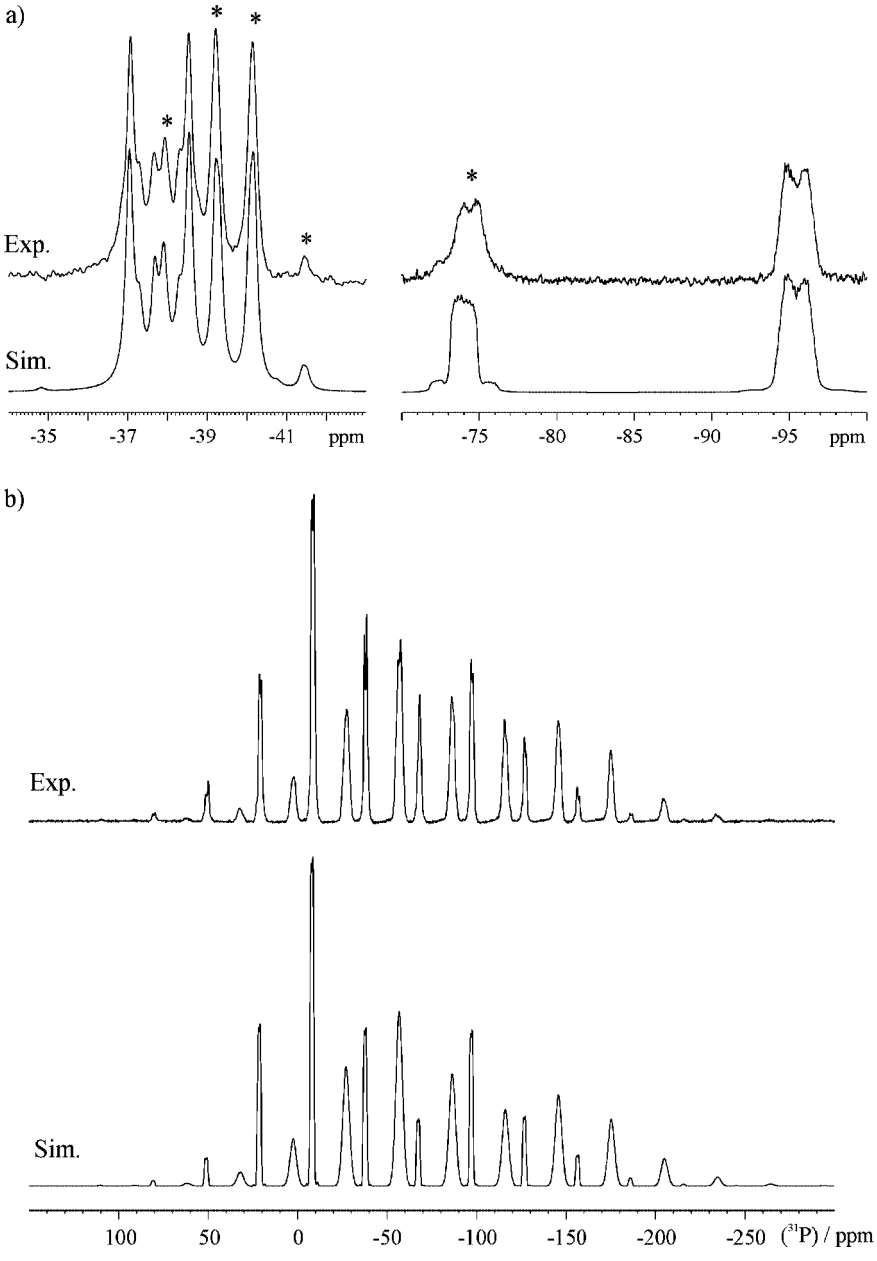

Figure 5. a) Experimental and simulated ^{31}P NMR spectra of $[Li_2(P_4Ph_4)(tmeda)_2]$ (**4**) and **4′′** (marked with asterisks) in toluene solution at T = 248 K. Chemical shifts and coupling constants are given in Table 3. b) ^{31}P CMAS spectrum of $[Li_2(P_4Ph_4)(tmeda)_2]$ (**4**). Top: experimental spectrum at 6000 Hz rotation frequency. Bottom: simulated spectrum with: $P^{2,3}$: $\delta_{iso} = -38.0$, $\delta_{11} = 33$, $\delta_{22} = 13$, $\delta_{33} = -159$ ppm; $P^{1,4}$: $\delta_{iso} = -86.3$, $\delta_{11} = 20$, $\delta_{22} = -62$, $\delta_{33} = -217$ ppm.

δ = –38.0 for $P^{2,3}$ and δ = –95.1 ppm for $P^{1,4}$. The X part is observed in the ^{7}Li NMR spectrum, where a slightly broadened triplet at δ = 10.9 ppm is observed ($^1J_{Li,P}$ = 37 Hz).

The resonances of the protons in the *para*-position of the phenyl rings are sharp, whereas those of the *ortho*- and *meta*-protons are broadened at low temperature. This is probably due to hindered rotation of the phenyl groups in **4**. This species corresponds to the ion triple with a structure close to that observed in the solid state.

This is further bolstered by the solid-state ^{31}P CPMAS spectrum of **4** (Figure 5, b). Only one species is present in the isolated crystalline material. The observation of only two isotropic chemical shifts (δ_{iso} = –38.0 and –86.3 ppm for the central and terminal P spins, respectively) is in agreement with the crystallographic C_2 symmetry of the ion triple **4** (see Figure 4). The principal elements of the chemical shift tensor, δ_{11} = 33, δ_{22} = 13, δ_{33} = –159 and δ_{11} = 20, δ_{22} = –62, δ_{33} = –217 ppm were obtained by a Herzfeld–Berger[11] analysis of the intensities of the spinning side-bands and refined by spectral simulation using the SIMPSON package.[12] It should be noted that the fine structure observed in the resonances shown in Figure 5 (b) is a consequence of orientation-dependent cross-terms involving the scalar and dipolar coupling and the chemical shift interactions and depends significantly on the frequency of magic angle spinning.[13] For the purpose of spectral simulation, phosphorus–phosphorus scalar coupling constants were taken into account as their isotropic solution values (Table 3) but were not refined, and coupling to the lithium isotopes was accounted for by processing with an appropriate Gaussian line-shape function.

It is interesting to note that while the isotropic chemical shifts of the central phosphorus atoms (δ_{iso} = –38.0 ppm) are equal, those of the terminal ones differ (δ_{iso} = –86.3 and –95.1 ppm in the solid state and solution, respectively). As there is no doubt about the constitution of **4** − in both cases the compound exists as the ion triple − we assume a slightly different conformation in solution, which might be due to loss of the Li–C_{ipso} interaction present in the solid phase.

The other species (**4′′**) observed in [D_8]toluene solution at 248 K also shows an AA′BB′X spin system (marked with asterisks in Figure 5a) with chemical shifts at δ = –39.7 ppm for $P^{2,3}$ and a broad resonance at δ = –74.4 ppm for $P^{1,4}$ in the ^{31}P NMR spectrum. For this species, no signal could be found in the ^{7}Li NMR spectrum.

Computations

Recently, Kaupp et al. have calculated the dependence of the $J_{P,P}$ coupling constants for the conformations **A** and **B** of the P_4 chain based on the experimentally known $M_2(P_4R_4)$ structures (Figure 6).[14] The coupling constants given in Table 3 depend on the alignment of nonbonding electron pairs at the phosphorus centers. In **A**, which has a small P–P–P–P torsion angle φ, the couplings follow the order $J_{1,4}$ (>300 Hz) >> $J_{1,3}/J_{2,4}$ (11–35 Hz), whereas in **B**,

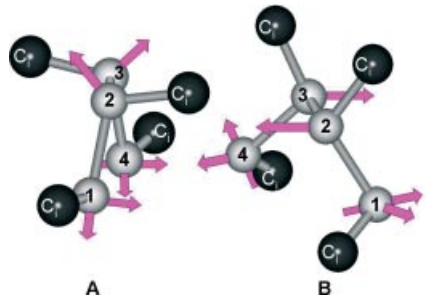

Figure 6. Conformations of the P_4 chains in tetraphosphanediides of type **A** {found in all $[M_2(P_4Ph_4)(solv)_x]$ with M = Li, Na, and $[Na_2(P_4tBu_4)(thf)_4]$} and **B** {observed in $[M_2(P_4Mes_4)(thf)_x]$ M = Na, x = 4; M = K, x = 6}. The *ipso* carbons of the aryl groups are indicated as C_i and the nonbonding electron pairs at the phosphorus centers are shown as magenta-colored arrows.

Table 3. Experimentally derived ^{31}P–^{31}P coupling constants [Hz] of the P^1–P^2–P^3–P^4 chain in **IIIa**,[5a] $[Na_2(P_4tBu_4)(thf)_4]$,[4] $[Na_2(P_4Mes_4)(thf)_4]$,[4] **4**, and **4′′**. The computed,[a] geometric, and magnetic properties for $Li_2(P_4H_4)_{opt}$,[b] $Na_2(P_4H_4)_{opt}$,[b] $Li_2(P_4Ph_4)(tmeda)_{2,cry,trunc}$,[c] and the $Li_2(tmeda)_1(P_4Ph_4)_{opt,trunc}$[c] isomers **A** and **B** are also given.

Entry		Type	P^1–P^2/P^3–P^4 [d]	$^1J_{1,2}/^1J_{3,4}$	P^2–P^3	$^1J_{2,3}$	φ	$J_{1,3}/J_{2,4}$	$P^1\cdots P^4$	$J_{1,4}$
Experimental										
1	$[Na_2(P_4Ph_4)(tmeda)_2]$ (**IIIa**)	A	2.160	–322	2.185	–306	20.3	–11	3.406	310
2	$[Na_2(P_4tBu_4)(thf)_4]$	A	2.169	–341	2.222	–306	8.8	–13	3.615	201
3	$[Na_2(P_4Mes_4)(thf)_4]$	B	2.165	–310	2.261	–118	72.7	120	4.247	3
4	$[Li_2(P_4Ph_4)(tmeda)_2]$ (**4**)	A	2.166	–271	2.190	–268	13.3	–35	3.229	310
5	**4′′**			–266		–15		67		280
Calculated										
6	$[Na_2(P_4H_4)]_{opt}$[b]	A	2.251	–200	2.248	–229	25.7	–26	3.644	292
7	$[Na_2(P_4Ph_4)(thf)_{2.5}]_{cry,trunc}$[14]	A	2.166	–304	2.207	–323	32.1	–21	3.486	432
8	$[Li_2(P_4H_4)]_{opt}$[b]	A	2.248	–190	2.252	–204	24.3	–22	3.414	320
9	$[Li_2(P_4Ph_4)(tmeda)_2]_{cry,trunc}$[a]	A	2.166	–267	2.190	–321	13.3	–29	3.229	529
10	$Li_2(tmeda)_1(P_4Ph_4)_{opt,trunc;}$ Isomer **A** [c]		2.215/2.231	–270/–259	2.254	–323	23.6	–27/–20	3.364	417
11	$Li_2(tmeda)_1(P_4Ph_4)_{opt,trunc;}$ Isomer **B**[c]		2.213	–305	2.262	–317	38.3	–25	3.451	323

[a] Coupling constants in Hz calculated at GIAO/B3LYP/6-311+G**//B3LYP/6-31G*.[15] [b] opt = properties of B3LYP/6-31G*-optimized structure. [c] trunc = truncated geometry; the NMR properties are calculated for the molecule where phenyl groups have been replaced by H atoms at a standard P–H distance of 1.427 Å and solvent molecules (tmeda) are omitted. [d] P^1–P^2 = P^3–P^4 if only one distance and $^1J_{1,2}$ = $^1J_{3,4}$ and $J_{1,3}$ = $J_{2,4}$ if only one coupling is given.

which has a large angle (>70°), a poor 1,4 alignment of the lone pairs causes the inverse ordering $J_{1,4}$ (<5 Hz) << $J_{1,3}$/$J_{2,4}$ (>100 Hz).

We performed the following computations:[15] i) ^{31}P chemical shifts were calculated at the GIAO/B3LYP/6-31G* level for a number of structural isomers of molecules of the general formula [$Li_2(P_4Ph_4)(tmeda)_n$] (n = 0, 1, 2). The values obtained for [$Li_2(P_4Ph_4)(tmeda)_2$] (**4**) with the structure observed in the crystal and with the optimized structure (B3LYP/6-31G*), denoted as $\mathbf{4}_{cry}$ and $\mathbf{4}_{opt}$, respectively, are δ = –108 ($\mathbf{4}_{cry}$, terminal), –52 ($\mathbf{4}_{cry}$, inner), –70 ($\mathbf{4}_{opt}$, terminal), and –17 ppm ($\mathbf{4}_{opt}$, inner), respectively. The chemical shift difference, $\Delta\delta$, between the terminal and the inner backbone ^{31}P nuclei is rather constant (–53 ppm relaxed and –56 ppm crystal geometry). The calculated data reproduce the experimental ones satisfactorily, which means that the chosen theoretical level is sufficient; ii) for comparison, the structures of the simple molecules [$Li_2(P_4H_4)$] and [$Na(P_4H_4)$] were optimized at the B3LYP/6-31G* level; iii) the ^{31}P–^{31}P coupling constants were calculated for model compounds in which the structure of the M_2P_4 core of the complete [$Li_2(P_4Ph_4)(tmeda)_n$] was maintained but the phenyl groups were replaced by hydrogen atoms and the tmeda molecules omitted. These truncated geometries are denoted as [$Li_2(P_4Ph_4)(tmeda)_n$]$_{trunc}$.

Table 3 lists the P–P coupling constants for the sodium tetraphosphanediides [$Na_2(P_4Ph_4)(tmeda)_2$] (**IIIa**),[5a] [$Na_2(P_4Ph_4)(thf)_5$] (**IIId**),[5] [$Na_2(P_4tBu_4)(thf)_4$],[4] and the lithium tetraphosphanediides **4** and **4′** as obtained by simulating the experimental spectra. The calculated data for $Li_2(P_4H_4)_{opt}$, $Na_2(P_4H_4)_{opt}$, [$Li_2(P_4Ph_4)(tmeda)_2$]$_{cry,trunc}$, and the isomers **A** and **B** of $Li_2(tmeda)(P_4Ph_4)_{opt,trunc}$ are given for comparison. We have also included the data of [$Na_2(P_4Ph_4)(thf)_{2.5}$]$_{cry,trunc}$ reported by Kaupp et al.[14]

The experimental data listed for compounds of structure type **A** show that the one-bond P–P couplings $^1J_{1,2}$ = $^1J_{3,4}$ are somewhat smaller for M = Li (entries 4, 5) than for M = Na (entries 1–3) and this trend is reproduced with the calculated model structures (entries 6–9). The $P^{1,2}$–$P^{3,4}$ bonds in the optimized models [$M_2(P_4H_4)$]$_{opt}$ (M = Li, Na) are longer than in the truncated structures [$M_2(P_4H_4)$]$_{trunc}$ and consequently the ^1J couplings are smaller. The $^1J_{2,3}$ coupling is influenced by both the P^2–P^3 distance and also by the dihedral angle φ. In compounds with structure **B** (entry 3), where φ is large, the $^1J_{2,3}$ coupling is rather small. As expected, the couplings $J_{1,3}$ = $J_{2,4}$ in the dilithium tetraphosphanediide [$Li_2(P_4Ph_4)(tmeda)_2$] (**4**) are in the range of the disodium compounds with the same structure type **A** and are smaller (entry 4) than for compounds with structure type **B** (entry 3). The $J_{1,4}$ coupling shows a dependency on the $P^1\cdots P^4$ distance and on the dihedral angle φ. At longer distances (>3.6 Å), $J_{1,4}$ decreases (compare entries 2 with entries 1 and 4). To some extent, this is also reflected by the calculations (compare entries 6 with 7 and 8 with 9). Especially small values for $J_{1,4}$ are observed for large torsion angles φ (entry 3). In agreement with the experiment, the calculated coupling constants for [$Na_2(P_4H_4)$]$_{opt}$ and [$Li_2(P_4H_4)$]$_{opt}$ show only little differences. Nevertheless, the difference $\Delta\delta$ = $\delta(P^1,P^4)$ – $\delta(P^2,P^3)$ between the calculated chemical shifts of the terminal and internal ^{31}P nuclei is strongly dependent on the alkali cation and significantly larger for Na [$Na_2(P_4H_4)$: $\Delta\delta$ = –176 ppm, with $\delta(P^1,P^4)$ = –232 and $\delta(P^2,P^3)$ = –56 ppm; $Li_2(P_4H_4)$: $\Delta\delta$ = –137 ppm, with $\delta(P^1,P^4)$ = –241 and $\delta(P^2,P^3)$ = –104 ppm]. It is noteworthy that the shifts of the atoms directly attached to the different cations are less affected than the remote phosphorus centers. Although much less pronounced, this is reflected by the experimental data {[$Na_2(P_4Ph_4)(tmeda)_2$] (**IIIa**): $\Delta\delta$ = –64.2 ppm with $\delta(P^1,P^4)$ = –89.1 and $\delta(P^2,P^3)$ = –24.9 ppm; [$Li_2(P_4Ph_4)(tmeda)_2$] (**4**): $\Delta\delta$ = –57.1 ppm, with $\delta(P^1,P^4)$ = –95.1 and $\delta(P^2,P^3)$ = –38.0 ppm}.

With respect to a possible structure for the second species **4′′** in solutions of **4**, the data in Table 3 give some hints: the slightly smaller $J_{1,4}$ and the positive $J_{1,3}$ = $J_{2,4}$ indicate that the conformation of the P_4 chain in **4′′** has a P–P–P–P torsion angle φ that is significantly larger than in **4** (>> 20°). The very small $^1J_{2,3}$ indicates that the P^2–P^3 bond may also be elongated. The fact that broadened ^{31}P NMR signals for the terminal phosphorus nuclei P^1, P^4 are observed and no ^{7}Li signal could be recorded even at low temperatures point to fast exchange processes. For the sodium compound, we have suggested previously the equilibrium [$Na_2(P_4Ph_4)(thf)_x$] ⇆ [$Na(thf)_y$]$^+$ + [$Na(P_4Ph_4)(thf)_z$]$^-$, (with δ_1 = –73.3, δ_2 = –30.8, δ_3 = –16.8, and δ_4 = –70.4 ppm and $^1J_{1,2}$ = 340, $^1J_{2,3}$ = 340, $^1J_{3,4}$ = 274, and $J_{2,4}$ = 148 Hz for the [$Na(P_4Ph_4)(thf)_z$]$^-$ anion).[5] A computational search of possible structures for a [$Li(P_4Ph_4)(thf)_z$]$^-$ anion only gave species with an almost co-planar P_4 chain and at least one significantly high-frequency-shifted resonance for an *internal* phosphorus nucleus (>39 ppm). This finding is not compatible with the experimental results, which show that the chemical shifts of the external ^{31}P nuclei in **4** and **4′′** are quite different. In view of the rather high ESP, it seems likely that **4′′** also has the structure of an ion triple with a strongly distorted P_4 chain. We therefore inspected various possible structures for **4′′** that contain only one tmeda molecule as co-ligand to lithium (Scheme 2).

Two isomers were found: isomer **A**, with a chelating tmeda molecule binding to only one Li ion in a κ^2-fashion, and isomer **B**, where the tmeda molecule bridges the two lithium ions in a μ_2-κ^1,κ^1-fashion. Isomer **A** is about 3 kcal mol^{-1} more stable than isomer **B**. The calculated (gas-phase) energies, ΔH_r, for the dissociation of one tmeda from **4** are in a reasonable range (21–24 kcal mol^{-1}; Scheme 2) to allow this process in solution. This idea is supported by measuring the diffusion coefficients of the $(P_4Ph_4)^{2-}$-containing species (0.26746×10^{-9} m^2 s^{-1}) and the tmeda molecules (0.29214×10^{-9} m^2 s^{-1}) by pulsed field gradient NMR techniques.[16] The significantly larger diffusion coefficient (ca. 10%) for the tmeda molecules is compatible with the dissociation process, [$Li_2(P_4Ph_4)(tmeda)_2$] ⇆ [$Li_2(P_4Ph_4)$-(tmeda)] + tmeda, where, on average, three tmeda molecule are coordinated and one tmeda molecule is free.

Indeed, the P–P–P–P torsion angle φ in **A** (23.6°) and especially **B** (38.3°) is somewhat larger than that observed in crystals (13.3°) and calculated (12°) for **4**. For isomer **A**,

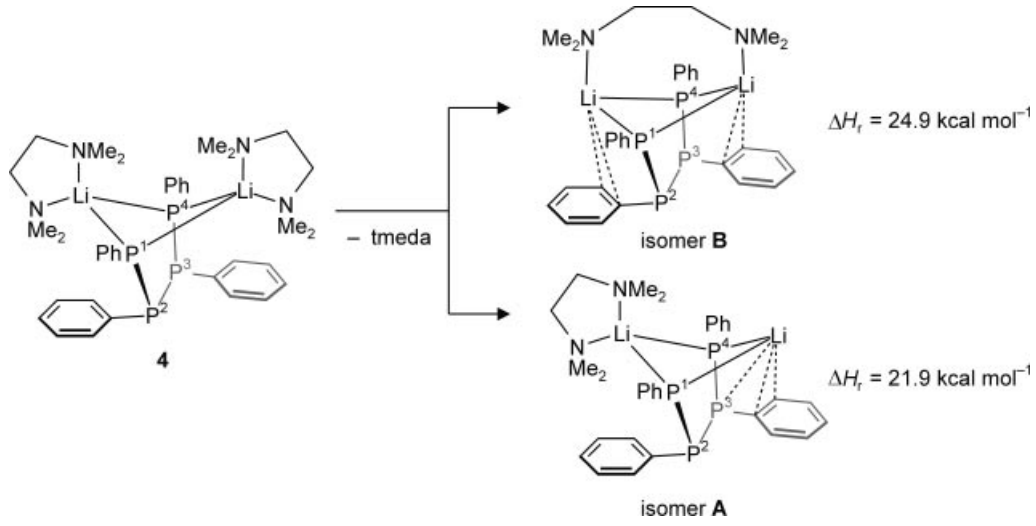

Scheme 2. Computed reaction enthalpies for the dissociation $[Li_2(P_4Ph_4)(tmeda)_2] \rightarrow [Li_2(P_4Ph_4)(tmeda)] + tmeda$.

the predicted ^{31}P chemical shifts are: P^1: δ = –74.03 ppm; P^2: δ = 6.87 ppm; P^3: δ = –28.52 ppm; P^4: δ = –30.06 ppm; and for the more symmetric isomer **B**: P^1,P^4: δ = –55 ppm; P^2,P^3: δ = 7 ppm. Considering that the equilibrium shown in Scheme 2 is likely to be fast on the NMR timescale, the chemical shift difference ($\Delta\delta$ = –42 ppm) between the averages of the chemical shifts for the external and internal ^{31}P nuclei, ½(P^1 + P^4) = –53 ppm and ½(P^2 + P^3) = –11 ppm, in isomer **A** fits better the experimental data for **4**′′ ($\Delta\delta$ = –34.7 ppm) than isomer **B** ($\Delta\delta$ = –62 ppm). However, the agreement between the calculated and experimental ^{31}P–^{31}P couplings is very poor (see Table 3) and at this point we cannot draw any definitive conclusion about the exact nature of **4**′′.

Conclusions

Optimized conditions for the selective syntheses of dilithium (*catena*-oligophosphane-α,ω-diides) $[Li_2(P_nPh_n)(solv)_x]$ have bee developed and the species with solv = tmeda and n = 2, 3, and 4 have been isolated as crystalline materials and structurally characterized. The compounds $[Li_2(P_2Ph_2)(tmeda)_2]$ and $[Li_2(P_4Ph_4)(tmeda)_2]$ form centrosymmetric genuine ion triples in the solid state and very probably also in solution. The lithium salt of the triphosphanediide behaves differently and is an ion pair, $[Li(tmeda)_2]^+[Li(P_3Ph_3)(tmeda)]^-$, in the solid and in solution. On average, the Li–P bonds (average of Li–P distances listed in Table 2: 2.55 Å) are 15% shorter than the Na–P distances (av. 2.98 Å) in comparable sodium oligophosphane-α,ω-diides (see Table 1). As a consequence, the electrostatic stabilization parameters, ESPs, of the lithium phosphanediides are significantly larger. Within its limits, this very simple model, which involves placing point charges at the positions of the cations and terminal phosphorus centers and neglecting all solvation energies and steric interactions, can be used to rationalize why $Li_2(P_2Ph_2)$ forms a simple ion triple while the sodium analogue forms a larger aggregate. Also, the fact that $[Na_2(P_3Ph_3)(solv)_x]$ forms an intact ion triple but the lithium analogue readily dissociates into an ion pair is expected. Specifically, the large drop of the ESP when going from the ion triple $[Na_2(P_3Ph_3)]$ (–0.79) to a hypothetical ion pair $[Na]^+$-$[Na(P_3Ph_3)]^-$ (ESP = –0.35; calculated with Na–P = 2.98 Å, P–P = 3.14 Å) cannot be overcompensated by the solvation of the dissociated Na^+ cation in an organic solvent. Further studies will concentrate on the question of whether these different aggregates also have different reactivity.

Experimental Section

General Techniques: All manipulations were performed under argon. All solvents were dried and purified using standard procedures and were freshly distilled under argon from sodium/benzophenone (THF, toluene, tmeda, dme, mtbe) or from sodium/diglyme/benzophenone (*n*-hexane) prior to use. Air sensitive compounds were stored and weighed in a glove box (Braun MB 150 B-G system) and reactions on small scale were performed directly in the glove box.

NMR Spectra were measured on Bruker AVANCE 500, 400, 300, and 250 systems. The chemical shifts (δ) are measured according to IUPAC[17] and expressed in ppm relative to TMS (^1H, ^{13}C), LiCl (^7Li), and H_3PO_4 (^{31}P). No satisfactory elemental analysis could be obtained due to the high air and moisture sensitivity of the compounds.

Solid State NMR: ^{31}P CP-MAS solid-state NMR spectra were acquired at room temperature on a Bruker Avance instrument operating at a ^1H Larmor frequency of 500 MHz. Conventional cross-polarization and magic-angle-spinning techniques were implemented using 4-mm rotors, with which rotational frequencies of more than 11 kHz were achieved. The ^{13}C carboxylate resonance of α-glycine appeared at δ = 176.0 ppm. As a consequence, referencing of all isotopes could be achieved as for the solution NMR using the unified Ξ scale.[17] Chemical shifts are expressed relative to H_3PO_4.

X-ray Crystallographic Investigations and Crystal Data: Data collection for the X-ray structure determinations were performed on

a Bruker SMART Apex diffractometer system with CCD area detector by using graphite-monochromated Mo-K_α (0.71073 Å) radiation and a low-temperature device. Crystals of $[Li_2(P_2Ph_2)(tmeda)_2]$ (**2**) suitable for X-ray diffraction were obtained by crystallization of a saturated toluene/tmeda solution at ambient temperature. Those of $[Li(tmeda)_2]^+[Li(P_3Ph_3)(tmeda)]^-$ (**3**) were grown from a toluene solution at 7 °C and of $[Li_2(P_4Ph_4)(tmeda)_2]$ (**4**) from a saturated mtbe solution at ambient temperature. In order to avoid quality degradation the single crystals were mounted in paraffin oil on top of a glass fiber and then brought into the cold nitrogen stream of a low-temperature device so that the oil solidified. All calculations were performed with SHELXTL (ver. 6.12) and SHELXL-97 (G.M. Sheldrick, Göttingen, 1997). The structures were solved by direct methods and successive interpretation of the difference Fourier maps, followed by full-matrix least-squares refinement (against F^2). Moreover, an empirical absorption correction using SADABS (ver. 2.03) was applied to all structures. All non-hydrogen atoms were refined anisotropically in the X-ray structures of $[Li_2(P_2Ph_2)(tmeda)_2]$ (**2**) and $[Li_2(P_4Ph_4)(tmeda)_2]$ (**4**), whereas the tmeda ligand in $[Li(tmeda)_2]^+[Li(P_3Ph_3)(tmeda)]^-$ (**3**) was refined isotropically. The ethylene bridge of the tmeda ligand is highly disordered on two positions and a large number (17) of restraints had to be used to achieve a satisfactory wR2 value. The contribution of the hydrogen atoms, in their calculated positions, was included in the refinement using a riding model for the X-ray structures of $[Li(tmeda)_2]^+[Li(P_3Ph_3)(tmeda)]^-$ (**3**) and $[Li_2(P_4Ph_4)(tmeda)_2]$ (**4**). Some hydrogen atoms of $[Li_2(P_2Ph_2)(tmeda)_2]$ (**2**) could be located in the Fourier difference map and hence were refined freely. The disordering in this molecule, which is caused by a flip of the Li–P–P–Li plane by 48° with respect to the Li–Li vector, was fixed using the bond lengths of the main structure, resulting in a large number (12) of restraints. The contribution of the hydrogen atoms of the disordered part was included by using a riding model. Upon convergence, the final Fourier difference map of all structures showed no significant peaks. Relevant data concerning crystallographic data, data collection, and refinement details are summarized in Table 4.

CCDC-280997 to -280999 (for **2**–**4**, respectively) contain the supplementary crystallographic data for this paper. These data can be obtained free of charge from The Cambridge Crystallographic Data Centre via www.ccdc.cam.ac.uk/data_request/cif

Computational Methods: Geometries were ab initio optimized[15] at the B3LYP/6-31G* level unless otherwise stated. Chemical shifts and nuclear spin-spin coupling constants were obtained for these geometries and truncated moieties by the GIAO/B3LYP/6-31G* method. The ^{31}P chemical shift of PH_3 (δ = 586 ppm) was calculated using a B3LYP/6-31G* structure at the GIAO/B3LYP/6-31G* level and set to –240 ppm vs. H_3PO_4 as the reference shift for all computed structures.

Synthesis of $[Li_2(P_2Ph_2)(tmeda)_2]$ (2): Lithium sand (39 mg, 5.62 mmol, 6 equivalents) and (P_5Ph_5) (500 mg, 0.925 mmol, 1 equiv.) were stirred for 24 h in THF (10 mL). The remaining lithium sand was filtered off and the solvent of the deep red filtrate was removed under high vacuum. The orange red powder was suspended in hot toluene (10 mL) and filtered off. The red powder was recrystallized from a hot mixture of toluene (4 mL) and tmeda (2 mL) and, on cooling to ambient temperature, the product separated as red crystals (673 mg, 63%). Red, very air-sensitive single crystals of $[Li_2(P_2Ph_2)(tmeda)_2]$ were obtained by storing a saturated toluene/tmeda solution at ambient temperature. $[Li_2(P_2Ph_2)(tmeda)_2]$ ($C_{24}H_{42}Li_2N_4P_2$, M = 462.45 g mol^{-1}): M.p. 151–153 °C (single crystal, uncorrected). ^{1}H NMR (500.23 MHz, [D$_8$]THF, 25 °C): δ = 2.18 [s, 8 H, $CH_{3(TMEDA)}$], 2.34 [s, 24 H, $CH_{2(TMEDA)}$], 6.33 (m, 2 H, *p*-H), 6.62 (m, 4 H, *m*-H), 7.26 ppm (m, 4 H, *o*-H). ^{7}Li NMR (194.4 MHz, DME/[D$_8$]toluene, 25 °C): δ = 0.6 ppm [s (br.)]. ^{13}C NMR (125.8 MHz, [D$_8$]THF, 25 °C): δ = 46.7 [s, $CH_{3(TMEDA)}$], 59.4 [s, $CH_{2(TMEDA)}$], 117.5 [s (br.), 4-C in Ph], 126.7 [t, ($^3J_{C,P}$ + $^4J_{C,P}$) = 2.4 Hz, 3,5-C in Ph], 131.0 [t, ($^2J_{C,P}$ + $^3J_{C,P}$) = 12.2 Hz, 2,6-C in Ph], 162.2 ppm [t, ($^1J_{C,P}$ + $^2J_{C,P}$) = 34.8 Hz, 1-C in Ph]. ^{31}P NMR (202.5 MHz, [D$_8$]THF, 25 °C): δ = –102.9 ppm (s).

Synthesis of $[Li(tmeda)_2]^+[Li(P_3Ph_3)(tmeda)]^-$ (3): Lithium sand (45 mg, 6.47 mmol; 3.5 equiv.) and (P_5Ph_5) (1.00 g, 1.85 mmol; 1 equiv) were stirred for 24 h in dme (10 mL). The orange precipitate was filtered off, washed with dme (2 mL), and dried in high vacuum. The light orange powder was dissolved in a mixture of toluene (5 mL) and tmeda (1 mL). The solvent was removed under

Table 4. Crystallographic data for compounds **2**, **3**, and **4**.

Compound	$[Li_2(P_2Ph_2)(tmeda)_2]$ (**2**)	$[Li(tmeda)_2]^+$ $[Li(P_3Ph_3)(tmeda)]^-$ (**3**)	$[Li_2(P_4Ph_4)(tmeda)_2]$ (**4**)
Empirical formula	$C_{24}H_{42}Li_2N_4P_2$	$C_{36}H_{63}Li_2N_6P_3$	$C_{36}H_{52}Li_2N_4P_4$
M	462.44	686.71	678.58
Crystal system	monoclinic	monoclinic	monoclinic
Space group	C_2/m (no. 12)	$P2_1/c$ (no. 14)	C_2/c (no. 15)
a [Å]	12.192(1)	13.283(1)	10.299(1)
b [Å]	14.059(1)	17.535(1)	17.644(1)
c [Å]	8.335(1)	18.331(1)	21.464(1)
β [°]	101.905(2)	99.828(2)	93.412(2)
V [Å^3]	1398.2(1)	4207.2(4)	3893.4(5)
μ [mm^{-1}]	0. 172	0.172	0.223
$D_{calcd.}$ [g cm^{-3}]	1.098	1.084	1.158
Crystal dimensions [mm]	0.52 × 0.45 × 0.34	0.24 × 0.13 × 0.05	0.14 × 0.13 × 0.10
Z	2	4	4
T [K]	100	100	200
$2\theta_{max}$ [°]	104.30	52.90	52.74
Reflections measured	22784	37854	14022
Reflections unique	8099 (R_{int} = 0.0191)	8646 (R_{int} = 0.0781)	3975 (R_{int} = 0.0505)
Parameters/restraints	184/12	377/17	212/0
$R1$ [$I \geq 2\sigma(I)$]	0.0411	0.0968	0.0594
$wR2$ (all data)	0.1260	0.2233	0.1391
Max./min. resid. e$^-$ dens. [e Å^{-3}]	1.035/–0.449	0.930/–0.747	0.355/–0.181

high vacuum to give a yellow powder (1.525 g, 72%). Yellow, very air-sensitive single crystals of $[Li(tmeda)_2]^+[Li(P_3Ph_3)(tmeda)]^-$ were obtained by storing a saturated toluene solution for several days at 7 °C. $[Li(tmeda)_2]^+[Li(P_3Ph_3)(tmeda)]^-$ ($C_{36}H_{63}Li_2N_6P_3$, M = 686.73 g mol^{-1}): M.p. 166 °C (single crystal, uncorrected). ^{1}H NMR (300.1 MHz, [D$_8$]toluene, 25 °C): δ = 1.92 [s (br.), 12 H, $CH_{2(TMEDA)}$], 2.03 [s (br.), 36 H, $CH_{3(TMEDA)}$], 6.87 (m, 1 H, *p*-H in Ph at P_A), 6.89 (m, 2 H, *p*-H in Ph at P_M), 6.97 (m, 2 H, *m*-H in Ph at P_A), 7.20 (m, 4 H, *m*-H in Ph at P_M), 8.04 (m, 4 H, *o*-H in Ph at P_M), 8.18 ppm (m, 2 H, *o*-H in Ph at P_A). ^{7}Li NMR (194.4 MHz, [D$_8$]toluene, –73 °C): δ = 11.4 [m (br.)], 10.5 ppm [s (br.)]. ^{13}C NMR (75.5 MHz, [D$_8$]toluene, 25 °C): δ = 45.9 [s, $CH_{3(TMEDA)}$], 57.2 [s, $CH_{2(TMEDA)}$], 120.0 (s, 4-C in Ph at P_M), 124.8 (s, 4-C in Ph at P_A), 127.4 (m, 3,5-C in Ph at P_A), 128.1 (m, 3,5-C in Ph at P_M), 130.0 (m, 2,6-C in Ph at P_M), 131.0 (m, 2,6-C in Ph at P_A), 155.8 (m, 1-C in Ph at P_M), 159.1 ppm (m, 1-C in Ph at P_A). Multiplets in the ^{13}C NMR spectra represent the X part of an AMM′X spin system. ^{31}P NMR (101.3 MHz, [D$_8$]toluene, 25 °C): δ = –52.3 [m, $^1J_{P(M),P(A)}$ = 223.8 Hz, A part of an AM_2 spin system, P_A], –71.5 ppm [m, $^1J_{P(M),P(A)}$ = 223.8 Hz, M part of an AMM′ spin system, $P_{(M+M')}$].

Synthesis of $[Li_2(P_4Ph_4)(tmeda)_2]$ (4): $[Li_2(P_3Ph_3)(dme)_x]$ (**3′**; 892 mg, 1.466 mmol, 5 equiv., x = 3) and (P_5Ph_5) (158 mg, 0.242 mmol, 1 equiv.) were suspended in Et_2O (30 mL). The yellow suspension was stirred for 24 h. The almost clear yellow solution was filtered through a Teflon filter. The solvent was removed under high vacuum and the obtained orange powder was dissolved in a mixture of toluene (10 mL) and tmeda (3 mL). The solvent was removed under high vacuum to give a yellow powder (865 mg, 87%). Slightly yellow, very air-sensitive single crystals of $[Li_2(P_4Ph_4)(tmeda)_2]$ were obtained by storing a saturated mtbe solution for several days at ambient temperature. $[Li_2(P_4Ph_4)(tmeda)_2]$ ($C_{36}H_{52}Li_2N_4P_4$, M = 678.6 g mol^{-1}): M.p. 174 °C (single crystals, uncorrected). ^{1}H NMR (500.2 MHz, [D$_8$]toluene, 25 °C): δ = 1.76 [s (br.), 8 H, $CH_{2(TMEDA)}$], 1.95 [s (br.), 24 H, $CH_{3(TMEDA)}$], 6.86 (m, 2 H, *p*-H in Ph at P_A), 7.02 (m, 2 H, *p*-H in Ph at P_B), 7.09 (m, 4 H, *m*-H in Ph at P_A), 7.14 (m, 4 H, *m*-H in Ph at P_B), 7.72 (m, 4 H, *o*-H in Ph at P_A), 8.22 ppm (m, 4 H, *o*-H in Ph at P_B). ^{7}Li NMR (194.4 MHz, [D$_8$]toluene, –25 °C): δ = 10.9 ppm (t, $^1J_{Li,P}$ = 37.3 Hz, 2 Li) ppm. ^{13}C NMR (125.8 MHz, [D$_8$]toluene, 25 °C): δ = 46.1 [s, $CH_{3(TMEDA)}$], 56.8 [s, $CH_{2(TMEDA)}$], 120.6 (s, 4-C in Ph at P_A), 125.7 (s, 4-C in Ph at P_B), 127.5 (s, 3,5-C in Ph at P_A), 127.6 (s, 3,5-C in Ph at P_B), 130.2 (m, 2,6-C in Ph at P_A), 133.9 (m, 2,6-C in Ph at P_B), 148.3 [m (br), 1-C in Ph at P_B], 154.3 ppm [m (br.), 1-C in Ph at P_A]. Multiplets in the ^{13}C NMR spectra represent the X part of an AA′BB′X spin system. ^{31}P NMR (202.5 MHz, [D$_8$]toluene, 25 °C): δ = –2.3 [m, $(PPh)_5$], –36.8 (br., $[Li_2(P_4Ph_4)(tmeda)_2]$), –53.3 (m, $[Li_2(P_3Ph_3)(tmeda)_3]$), –73.0 (m, $[Li_2(P_3Ph_3)(tmeda)_3]$), –76.0 (br., $[Li_2(P_4Ph_4)(tmeda)_2]$), –95.4 (br., $[Li_2(P_4Ph_4)(tmeda)_2]$) ppm. ^{31}P NMR (202.5 MHz, [D$_8$]toluene, –25 °C): δ = –38.0 (m, B part of an AA′BB′X_2 spin system, P_B [**4**]), –39.7 (m, B part of an AA′BB′X spin system, P_B [**4′′**]), –74.4 (m, A part of an AA′BB′X spin system, P_A [**4′′**]), –95.1 ppm (m, A part of an AA′BB′X_2 spin system, P_A [**4**]); ratio **4**/**4′′** = 100:81. ^{31}P{^{1}H} CPMAS (202.5 MHz, 25 °C): δ_{iso} = –38, $\delta_{11} \approx 50$, $\delta_{22} \approx -10$, $\delta_{33} \approx -155$ (B part); δ_{iso} = –87, $\delta_{11} \approx 0$, $\delta_{22} \approx -55$, $\delta_{33} \approx -205$ ppm (A part). ^{7}Li NMR (194.4 MHz, [D$_8$]toluene, –25 °C): δ = 10.9 ppm (t, $^1J_{Li,P}$ = 37.3 Hz, 2 Li).

Supporting Information (see footnote on the first page of this article): Plots of the ^{13}C NMR spectra of compounds **2**, **3**, and **4** and details of the simulation of the ^{31}P CP-MAS spectrum with the SIMPSON package.

Acknowledgments

This work was supported by Ciba Speciality Chemicals and the ETH Zürich.

[1] Z.-W. Wang, Li-S. Wang, *Green Chem.* **2003**, *5*, 737.
[2] Reviews: a) K. Issleib, *Z. Chem.* **1962**, *2*, 163; b) M. Baudler, K. Glinka, *Chem. Rev.* **1993**, *93*, 1623. The formation of cyclic oligophosphanes is described from $PhPCl_2$/Li in: c) P. R. Bloomfield, K. Parvin, *Chem. Ind.* **1959**, 541; from $PhPCl_2$/Na: d) F. Pass, H. Schindlbauer, *Monatsh. Chem.* **1959**, *90*, 148; e) L. Horner, P. Beck, H. Hoffmann, *Chem. Ber.* **1959**, *92*, 2088; f) W. Kuchen, H. Buchwald, *Chem. Ber.* **1958**, *91*, 2296; from $PhPCl_2$/Mg: g) W. A. Henderson, M. Epstein, F. S. Seichter, *J. Am. Chem. Soc.* **1963**, *85*, 2462; h) A. Hinke, W. Kuchen, *Chem. Ber.* **1983**, *116*, 3003; from $PhPCl_2$/Zn: i) M. Scherer, D. Stein, F. Breher, J. Geier, H. Schönberg, H. Grützmacher, *Z. Anorg. Allg. Chem.* **2005**, *631*, 2770; j) H. Grützmacher, J. Geier, H. Schönberg, M. Scherer, D. Stein, S. Boulmaâz, WO2004/050668.
[3] $[M_2(P_nPh_n)]$, M = Li–Cs, n = 3, 4: a) P. R. Hoffman, K. G. Caulton, *J. Am. Chem. Soc.* **1975**, *97*, 6370; b) M. Baudler, D. Koch, *Z. Anorg. Allg. Chem.* **1976**, *425*, 227; $[M_2(P_3Ph_3)]$, M = Na, K: c) M. Baudler, D. Koch, E. Tolls, K. M. Diedrich, B. Kloth, *Z. Anorg. Allg. Chem.* **1976**, *420*, 146; $[Na_2(P_2Ph_2)]$: d) J. W. B. Reesor, G. F. Wright, *J. Org. Chem.* **1957**, *22*, 385; $[Li_2(P_2Ph_2)]$ and $[K_2(P_2Ph_2)]$: e) K. Issleib, K. Krech, *Chem. Ber.* **1966**, *99*, 1310; $PhPNa_2$ has been assumed to be a by-product in the reaction of $(PhP)_n$ with sodium: f) W. Kuchen, H. Buchwald, *Chem. Ber.* **1958**, *91*, 2296; $[Na_2(tBu_3Si–P–P=P–P–SitBu_3)]$: g) N. Wiberg, A. Wörner, K. Karaghiosoff, D. Fenske, *Chem. Ber./Recueil* **1997**, *130*, 135.
[4] R. Wolf, A. Schisler, P. Lönnecke, C. Jones, E. Hey-Hawkins, *Eur. J. Inorg. Chem.* **2004**, 3277.
[5] a) J. Geier, H. Rüegger, M. Wörle, H. Grützmacher, *Angew. Chem.* **2003**, *115*, 4081; *Angew. Chem. Int. Ed.* **2003**, *42*, 3951; b) J. Geier, J. Harmer, H. Grützmacher, *Angew. Chem.* **2004**, *116*, 4185–4189; *Angew. Chem. Int. Ed.* **2004**, *43*, 4093–4097c) D. Stein, J. Geier, H. Schönberg, H. Grützmacher, *Chimia* **2005**, *59*, 119.
[6] A. Streitwieser Jr, *Acc. Chem. Res.* **1984**, *17*, 353.
[7] N. Korber, J. Aschenbrenner, *J. Chem. Soc., Dalton Trans.* **2001**, 1165.
[8] Compare, for example, the molar enthalpy of solution for LiCl (–37.03 kJ mol^{-1}) and NaCl (3.88 kJ mol^{-1}).
[9] H. Bock, C. Nather, Z. Havlas, A. John, C. Arad, *Angew. Chem.* **1994**, *106*, 931; *Angew. Chem. Int. Ed. Engl.* **1994**, *33*, 875.
[10] For the structure of [K(18-C-6)][NHPh] see: P. B. Hitchcock, A. V. Khvostov, M. F. Lappert, A. V. Protchenko, *J. Organomet. Chem.* **2002**, *647*, 198 and references cited therein.
[11] J. Herzfeld, A. E. Berger, *J. Chem. Phys.* **1980**, *73*, 6021.
[12] M. Bak, J. T. Rasmussen, J. C. Nielsen, *J. Magn. Reson.* **2000**, *147*, 296.
[13] G. Wu, B. Sun, R. E. Wasylishen, R. G. Griffin, *J. Magn. Reson.* **1997**, *124*, 366.
[14] M. Kaupp, A. Patrakov, R. Reviakine, O. L. Malkina, *Chem. Eur. J.* **2005**, *11*, 2773.
[15] M. J. Frisch, G. W. Trucks, H. B. Schlegel, G. E. Scuseria, M. A. Robb, J. R. Cheeseman, J. A. Montgomery Jr, T. Vreven, K. N. Kudin, J. C. Burant, J. M. Millam, S. S. Iyengar, J. Tomasi, V. Barone, B. Mennucci, M. Cossi, G. Scalmani, N. Rega, G. A. Petersson, H. Nakatsuji, M. Hada, M. Ehara, K. Toyota, R. Fukuda, J. Hasegawa, M. Ishida, T. Nakajima, Y. Honda, O. Kitao, H. Nakai, M. Klene, X. Li, J. E. Knox, H. P. Hratchian, J. B. Cross, C. Adamo, J. Jaramillo, R. Gomperts, R. E. Stratmann, O. Yazyev, A. J. Austin, R. Cammi, C. Pomelli, J. W. Ochterski, P. Y. Ayala, K. Morokuma, G. A. Voth, P. Salvador, J. J. Dannenberg, V. G. Zakrzewski, S. Dapprich, A. D.

Daniels, M. C. Strain, O. Farkas, D. K. Malick, A. D. Rabuck, K. Raghavachari, J. B. Foresman, J. V. Ortiz, Q. Cui, A. G. Baboul, S. Clifford, J. Cioslowski, B. B. Stefanov, G. Liu, A. Liashenko, P. Piskorz, I. Komaromi, R. L. Martin, D. J. Fox, T. Keith, M. A. Al-Laham, C. Y. Peng, A. Nanayakkara, M. Challacombe, P. M. W. Gill, B. Johnson, W. Chen, M. W. Wong, C. Gonzalez, J. A. Pople, *Gaussian 03*, revision C.02, Gaussian, Inc., Wallingford CT, **2004**.

[16] M. Valentini, H. Rüegger, P. S. Pregosin, *Helv. Chim. Acta* **2001**, *84*, 2833.

[17] R. K. Harris, E. D. Becker, S. M. Cabral de Menezes, R. Goodfellow, P. Granger, *Pure Appl. Chem.* **2001**, *73*, 1795.

Received: April 26, 2006
Published Online: August 18, 2006

